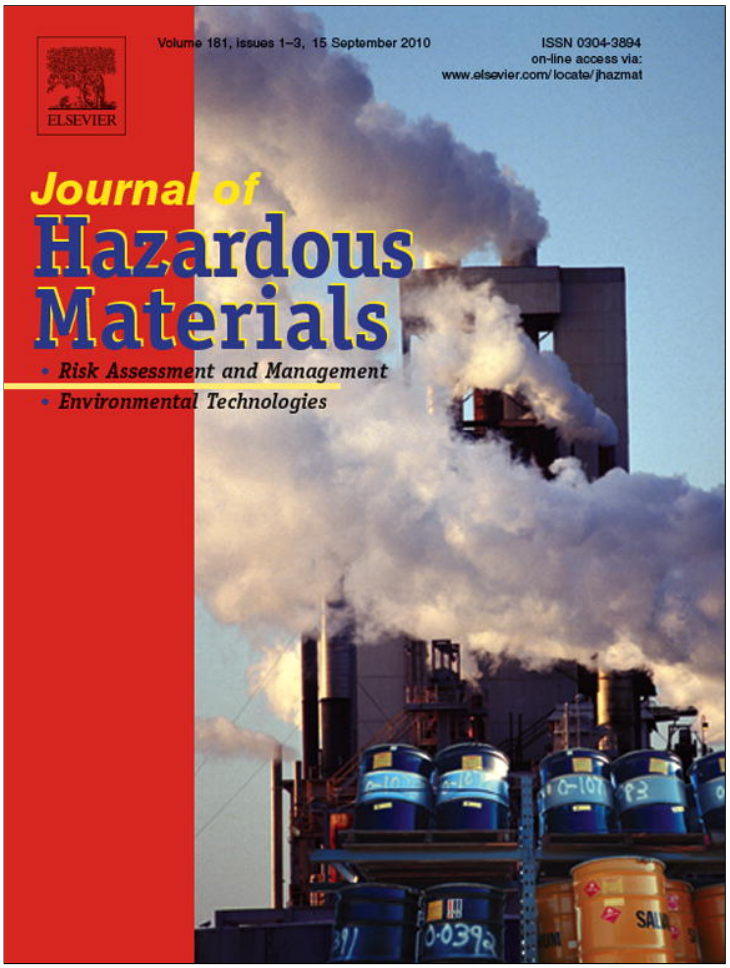

Journal of Hazardous Materials 181 (2010) 375–381

Contents lists available at ScienceDirect

Journal of Hazardous Materials

journal homepage: www.elsevier.com/locate/jhazmat

# On the use of magnetic nano and microparticles for lake restoration

Inmaculada de Vicente[a,b,*], Azahara Merino-Martos[b], Luis Cruz-Pizarro[a,b], Juan de Vicente[c]

[a] Departamento de Ecología, Facultad de Ciencias, Universidad de Granada, Granada 18071, Spain
[b] Instituto del Agua, Universidad de Granada, Granada 18071, Spain
[c] Departamento de Física Aplicada, Facultad de Ciencias, Universidad de Granada, Granada 18071, Spain

ARTICLE INFO

*Article history:*
Received 1 February 2010
Received in revised form 8 April 2010
Accepted 5 May 2010
Available online 11 May 2010

*Keywords:*
Phosphorus
Magnetic particles
Lake restoration
Eutrophication

ABSTRACT

Innovative approaches are of outstanding importance to devise technologies for dealing with eutrophication of inland waters. This study provides a quantitative estimate showing the convenience of using magnetic nano- and micronsized particles as phosphate absorbents and their later removal from solution by high gradient magnetic separation. Two different materials are investigated (iron and magnetite) having a controlled shape and size well in the colloidal domain. Magnetite particles adsorb more phosphate (empirical saturation constant = 27.15 mg P $g^{-1}$ Fe) than iron particles (empirical saturation constant = 18.83 mg P $g^{-1}$ Fe) as a consequence of the different particle size (average values for particle diameters of 90.6 ± 1.2 and 805 ± 10 nm for magnetite and for iron, respectively). A protocol is established for the successful reutilization of these magnetic particles by repeated washing with NaOH and therefore, optimizing the economic cost of this technology. Magnetic particles are also surface treated with amino silane groups (APTS) to counteract magnetic and van der Waals attractive interactions and promote kinetic stability. APTS-coated iron particles experience a notable increase in phosphate maximum adsorption capacity which could be explained by a remarkable increase in electrophoretic mobility. We propose the use of APTS-coated iron particles which are less-expensive and easy to obtain as a promising technique for lake restoration.



## 1. Introduction

Eutrophication, an increased primary productivity (trophy) in a water body due to enhanced availability or usage nutrients, has resulted in a deterioration of lake ecosystems worldwide [1–3]. Visible indications of eutrophication are high turbidity caused by algal blooms, reduced or absent submerged vegetation, mass development of harmful cyanobacteria (blue green algae), reduced species diversity, oxygen depletion, formation of hydrogen sulfide, fish kills and smell nuisance [4]. As a consequence, changing lake's productivity, the biology of the lake is drastically affected as a whole. In most inland waters the nutrient phosphorus (P) is the minimum factor controlling the degree of eutrophication and, due to the strong relationship between total P concentrations and chlorophyll reducing the P concentrations in the lake water is the most important strategy for eutrophication control.

The P availability in the lake water can be decreased by reducing P input, increasing P retention in the sediment or increasing P export. Among them, the careful management and control of P loading has been adopted worldwide as the keystone and centerpiece of eutrophication management [5]. Additionally, to reinforce recovery, various physical and chemical methods have been employed to combat the internal P loading, including sediment dredging and oxygenation of the hypolimnion with pure oxygen or nitrate, among others. Finally, biological tools such as biomanipulation comprising removal of planktivorous fish and/or stocking of piscivorous fish, are frequently used for lake restoration especially in North Europe [6–8]. Overall, reduction in P inputs is essential for lake restoration before considering increasing P retention in the sediment or increasing P export. In fact, the absence of long-term effects (>8–10 years) of lake restoration is frequently caused to insufficient external P loading reduction.

New and innovative methods are of great importance to devise technologies for dealing with environmental problems. The application of magnetic particle technology to solve environmental problems is one of these methods that have received considerable attention in recent years (i.e. [9,10]). Magnetic particles can be used to adsorb contaminants from aqueous or gaseous effluents and after the adsorption is carried out, the adsorbent can be separated from the medium by a simple high gradient magnetic separation process. Some examples of this technology are the use of magnetite particles to accelerate the coagulation of sewage [11], the removal of divalent metals from wastewater [9,10], the use of magnetite-coated functionalized polymer such as resin to remove radionuclides from milk [12], the use of poly(oxy-2,6-dimethyl-1,4-

* Corresponding authors at: Water Research Institute, University of Granada, Ramon y Cajal 4, 18071, Granada, Spain. Tel.: +34 958248323; fax: +34 958243093.
*E-mail address:* ivicente@ugr.es (I. de Vicente).

0304-3894/$ – see front matter © 2010 Elsevier B.V. All rights reserved.
doi:10.1016/j.jhazmat.2010.05.020

phenylene) for the adsorption of organic dyes [13], and the use of polymer-coated magnetic particles for oil spill remediation [14].

Hence, as an alternative technology, magnetic separation of precipitated P could be considered as a promising tool for lake restoration. Several outstanding advantages of using these particles for lake restoration can be suggested: (i) the recovery of magnetic particles from the solution, reducing both the effects in the aquatic biota and the economic costs and (ii) the reusability of the particles, thus reducing economic costs.

In this context, the main purpose of the present paper was to achieve the convenience of using well-controlled magnetic adsorbents to retain P and its later removal from lake water by a simple magnetic separation procedure after saturation is reached. To do so, a set of laboratory experiments were carried out in order to select the more appropriate conditions for increasing the efficiency of P adsorption onto two types of magnetic particles (micronsized iron and nanosized magnetite particles). Firstly, the P adsorption capacity of bare magnetic particles is evaluated and the effect of particle size investigated. Since the applicability of magnetic particles as adsorbents depends not only on their adsorption capacity but also on their reusability, a protocol is established here to desorb P from the particles. Finally, particles are functionalized by using aminopropyl-triethoxysilane (APTS), and hence positively charging the particles, to ascertain the effect of electrostatic interactions in the adsorption process.

## 2. Magnetic separation technique

The behavior of a small piece of magnetic material under the presence of a magnetic field strongly depends on the typical size. Very small particles (less than a few nanometers diameter) behave as magnetic monodomains. Since Brownian motion is very significant for such small systems, particles are stable in a magnetic field gradient and do not aggregate.

On the other hand, larger magnetic particles consist of magnetic multidomains. In the presence of an external magnetic field, these particles become magnetized. As a consequence two kinds of interactions come into play: particle-particle and particle-field interactions [15]. In this work we are concerned about the second kind of interaction, particle-field interactions, which are described by the following equation:

$$\underline{F_m} = (\underline{m} \cdot \underline{\nabla})\underline{B} \tag{1}$$

where $\underline{B}$ is the magnetic induction, and $\underline{m}$ is magnetic particle dipole moment. Assuming that the particles are dispersed in a non magnetic medium, their magnetic dipole moment can be written as $\underline{m} = V\chi\underline{H}$, where $V$ is the particle volume, $\underline{H}$ is the magnetic field strength and $\chi$ is the magnetic susceptibility of the particles.

For the case of a dilute suspension, the permeability of the suspension is not too different from the one of vacuum and $\underline{B} = \mu_0\underline{H}$. Bearing this in mind, the magnetic force on the particle can be written as:

$$\underline{F_m} = \frac{V\chi}{\mu_0}(\underline{B} \cdot \underline{\nabla})\underline{B} \tag{2}$$

If there are no time-varying electric fields or currents in the medium, $\underline{\nabla} \times \underline{B} = 0$ and the magnetic force can be manipulated to give:

$$\underline{F_m} = V\chi\nabla\left(\frac{1}{2}\underline{B} \cdot \underline{H}\right) \tag{3}$$

where $1/2\underline{B} \cdot \underline{H}$ is the magnetostatic field energy density. Thus, if $\chi > 0$ the magnetic force acts in the direction of steepest ascent of the energy density scalar field. This is the reason why iron filings are brought near the pole of a magnet, they are attracted towards that pole. It is also the basis for any magnetic separation application. As observed from Eq. (3), larger forces are achieved for larger particles having large magnetic susceptibility. Hence, one may think that large magnetic particles are the most convenient ones.

Magnetic separation is always a two-step process, involving (i) the adsorption, tagging or labeling of the desired material with magnetic particles, and (ii) the separating out of these entities via a magnetic separation device. The simplest magnetic separator is a permanent magnet. However, faster accumulation rates can be obtained by using other more complicated devices [16,17].

## 3. Experimental

### 3.1. Materials

Micronsized iron (Fe) particles were kindly supplied by BASF (Germany) and used without further treatment to make the suspensions. According to the manufacturer, the composition of this powder is 97.5% iron, 0.9% carbon, 0.5% oxygen, and 0.9% nitrogen.

All chemicals were analytical quality. KOH (90% purity), $KNO_3$, $FeSO_4{\cdot}7H_2O$ (extra pure), and APTS were obtained from Sigma–Aldrich (Spain), $KH_2PO_4$, $NaHCO_3$, NaOH and HCl were obtained from Panreac (Spain). Deionized and filtered water (Milli-Q Academic, Millipore, France) was used in the preparation of all the suspensions

### 3.2. Synthesis of magnetite nanoparticles

Nanometer sized magnetite ($Fe_3O_4$) particles are frequently prepared by stoichiometric coprecipitation of $Fe^{2+}$ and $Fe^{3+}$ salts in basic medium [18]. Unfortunately, such small particles are not interesting for us since thermal Brownian motion overcomes magnetic forces [19], which means that these particles could not be magnetically separated from solution. However, larger magnetite particles can be prepared from slow oxidation of $Fe(OH)_2$ by nitrate ions under controlled atmosphere [20]. This approach has been successfully applied in the past for the preparation of other iron oxides as well [21].

Magnetite particles having a typical size of 100 nm diameter were prepared following a sol–gel precipitation and re-crystallization method involving an iron hydroxide gel formation followed by aging under nitrate ions. To this end a 1 L five-necked sealed jacketed reactor was used to accurately control experimental conditions. The synthesis requires inert atmosphere and this is achieved through displacement of dissolved oxygen by nitrogen. The reaction temperature was fixed at 85 °C.

Several stock solutions were initially prepared consisting of 0.2 M $KNO_3$, 0.005 M KOH and 0.03 M $FeSO_4{\cdot}7H_2O$. Water used in the preparation of the stock solutions was previously subjected to nitrogen flow in order to displace dissolved oxygen. The synthesis process involved the mixing of 250 mL KOH, 100 mL $KNO_3$ and 550 mL $H_2O$ solutions in the reactor under agitation and nitrogen flow. Then, 100 mL $FeSO_4{\cdot}7H_2O$ were added. Just immediately after $Fe^{2+}$ salt addition, a sudden color change was observed due to the formation of iron hydroxide. After 4 h under nitrogen flow at 85 °C, the reaction was stopped in ice water. Decantation in the presence of a permanent magnet (405 mT) placed at the bottom of the container, and redispersion in Milli-Q water, was the method used to clean the suspension of unreacted ions. This process was repeated 5 or 6 times until the supernatant thus obtained was transparent and had low electric conductivity (<2 μS/cm). Particles were kept in a fridge in ethanol for later use. In order to get the dry weight, magnetite/ethanol dispersions were placed in Petri disks in a convection oven at 60 °C for 24 h. The black sediment obtained was later analyzed. The yield of this reaction is 1.4 g of magnetite per litre of initial solution.

### 3.3. Electron microscopy of the magnetic particles

Particle morphology was studied in a LEO Gemini 1530 field-emission scanning electron microscope (FESEM) operating in a secondary electron (SE) mode. Microscope samples were prepared by drying on top of a glass substrate a droplet of a suspension of the magnetic particles dispersed in ethanol. A thin (ca. 20 nm) coating of carbon was then applied.

### 3.4. Magnetic characterization of Fe and $Fe_3O_4$ powders

The magnetization ($M$) of the powder magnetic particles was measured as a function of the external applied magnetic field ($H$) using a Quantum Design (San Diego, CA) MPMS-XL 5.0 Tesla Magnetometer. The external field was swept from −4000 to 4000 kA $m^{-1}$. Experiments were run at room temperature. Saturation magnetization was obtained by extrapolation to zero the magnetization values in the high field range versus the inverse of the applied magnetic field strength.

### 3.5. Electrokinetic characterization

Electrophoretic mobility ($\mu_e$) was measured with a Zeta-PALS (Brookhaven) at 25.0 ± 0.5 °C. Measurements were carried out 24 h after preparation of the suspensions, and the pH was readjusted immediately before measuring mobility. Every mobility data point presented in this work is the average of 10 measurements taken for the same sample in the course of a 'run'. The error bars are given by the standard deviation of those five measurements. Because of the high density of the particles and therefore their tendency to sediment under gravity, the samples were sonicated for 5 min and the measuring cell was turned over a couple of times before every run. As a preliminary step, the dependence of the measured mobility on the solid-phase concentration of our suspensions was first investigated. At low solid concentration, mobility increased with particle concentration and then remained practically constant for concentrations over 0.05 g $L^{-1}$. Results shown here correspond to suspensions having 1 g $L^{-1}$ of particles content.

### 3.6. Preparation of magnetic suspensions

The preparation of the suspensions consisted of the following steps. (i) 10 g of magnetic powder and 200 mL of purified water were mixed in a polyethylene container. (ii) The mixture was stirred first by hand, and then in an ultrasonic bath. (iii) Step (ii) was repeated several times and, finally, the sample was immersed in a Branson sonifier (model 450) to ensure the required final homogeneity. The gradual homogenization of the samples was confirmed by the disappearance of the aggregates initially observed in the container bottom. As 1 mL of the stock Fe solution (50 g $L^{-1}$) was added up to a final volume of 50 mL, the final Fe concentration was 1 g $L^{-1}$, similarly to that reported by Karapinar et al. [22].

### 3.7. Effect of pH in the adsorption by Fe particles

Firstly, the effect of pH on P adsorption by Fe particles was investigated. To this end, 1 mL of the stock Fe suspension (50 g $L^{-1}$) and 1 mL of 5 mM $KH_2PO_4$ solution were added to 40 mL of 3 mM $NaHCO_3$ (acting as pH buffer) in 50 mL centrifuge tubes. Afterwards, pH was adjusted to the desired value, and then the suspensions were left for shaking in a horizontal shaker during 24 h at 20 °C (150 rpm). After that time, pH was readjusted and made up to 50 mL of volume with 3 mM $NaHCO_3$. Thus, the initial Soluble Reactive Phosphorus (SRP) concentration in the centrifuge tube was fixed to 100 μM P. Next, magnetic particles were separated from the suspension by applying a magnetic field gradient of approximately 12 400 kA $m^{-2}$ during 5 min (PASCO scientific; EM-8641). The supernatant was pipetted off and filtered (Whatman GFF) to be analyzed for molybdenum reactive P using the spectrophotometric procedure by Murphy and Riley [23]. The whole process was repeated for different pH's in the range from pH 5 to pH 9.

### 3.8. Adsorption isotherm for Fe and $Fe_3O_4$

Adsorption experiments were carried out in batch mode by adding 1 mL of the stock Fe or $Fe_3O_4$ suspensions to 45 mL 3 mM $NaHCO_3$ in 50 mL centrifuge tubes. Afterwards, the samples were shaken for 24 h and later, 1 mL of $KH_2PO_4$ solutions with concentrations ranging from 5 to 60 mM P was added to each tube. Once the pH of the suspensions was adjusted to 7.0 ± 0.3, they were shaken for 24 h. After adjusting again the pH to 7.0 ± 0.3, suspensions were transferred to 50 mL volumetric flasks and made up to volume with 3 mM $NaHCO_3$. Thus, the initial SRP concentrations varied between 0.1 and 1.2 mM. The next step was the filtration of the suspension in order to evaluate the amount of P adsorbed onto the magnetic particles. This process closely follows that described in section above.

### 3.9. Reusability of magnetic micro and nanoparticles

A new set of adsorption experiments was performed to test the possible reutilization of iron and magnetite particles. Once a typical adsorption experiment is carried out as described above, magnetic particles were separated and later washed twice with 1 M NaOH and three more times with 3 mM $NaHCO_3$. Resulting particles were then dried in Petri disks in a convection oven at 60 °C for 24 h and ready for later usage.

### 3.10. Adsorption by magnetic functionalized particles

Magnetic particles were surface treated to improve P adsorption at neutral pH following a similar procedure as described by del Campo et al. [24]. Concretely, 1.25 g of magnetic particles were dispersed in 25 mL of APTS (2%, v/v). As del Campo et al. [24] noticed, there exists a clear change in the density of active amine groups with the reaction time, reaching the maximum density after 20 h shaking. Accordingly, in this study, suspensions of magnetic particles were left for shaking during 24 h. Afterwards, suspensions were centrifuged (20,000 rpm, 5 min) and the supernatants withdrawn. Pellets were washed 5 times as follows: (i) addition of 25 mL of 3 mM $NaHCO_3$, (ii) sonication for 5 min, (iii) shaking for 10 min and (iv) centrifugation for 5 min (20,000 rpm). The final pellet was diluted and sonicated in 30 mL of 3 mM $NaHCO_3$. Once the suspensions were shaken for 24 h, they were ready for being used for adsorption experiments by following the same methodology explained in sections above.

## 4. Data analysis

### 4.1. Adsorption models

The equilibrium adsorption capacity of phosphorous, $q$, is calculated as follows:

$$q = \frac{C_0 - C_e}{M_a} V \quad (4)$$

where $C_0$ represents the initial P concentration in solution (mg $L^{-1}$), $C_e$ is the final or equilibrium concentration (mg $L^{-1}$), $M_a$ is the mass of adsorbent used in grams (in this case Fe or $Fe_3O_4$) and $V$ is the total volume of solution (L).

**Table 1**
Fitting parameters to a Log-normal distribution. $e^{\mu}$ represents the center of the distribution and $\sigma$ represents the width of the distribution.

| | Median, $e^{\mu}$ (nm) | Standard deviation, $\sigma$ (nm) |
|---|---|---|
| Iron | 805 ± 10 | 0.36 ± 0.01 |
| Magnetite | 90.6 ± 1.2 | 0.194 ± 0.012 |

The maximum adsorption capacity was estimated here according to the one layer Langmuir model [25]:

$$q = \frac{K_L M_L C_e}{1 + K_L C_e} \quad (5)$$

where $K_L$ is an adsorption constant related to the binding energy ($L\,g^{-1}$) and $M_L$ is an empirical saturation constant, that is the maximum mass of solute adsorbed per unit mass of adsorbent (adsorption capacity) ($mg\,g^{-1}$). $K_L$ and $M_L$ were empirically determined from the linear forms of the Langmuir model. It is important to note that assumptions used to derive the Langmuir equation are rather stringent [26]. For example, ideal behavior on the surface implies a homogeneous surface that lacks dislocations or any other structural nonidealities that might induce preferred adsorption. In addition, it assumes that a monolayer of adsorbed molecules is formed on the surface and an adsorption maximum is achieved as the monolayer becomes filled by the adsorbate. Although it is difficult to realize these conditions in practice, the Langmuir isotherm provides a conceptual basis for thinking about surface adsorption as well as a basis for modelling the adsorption process. Furthermore, the equation makes a convenient form for fitting data because it accommodates many situations in which the Langmuir model assumptions do not strictly apply [27].

### 4.2. Statistical analysis

All experiments reported in this work were run in triplicates. Comparison of mean values was done using Student's *t*-test and, unless otherwise stated, $p < 0.05$ is considered statistically significant. Statistical analyses were performed using Statistica 6.0 Software [28].

## 5. Results and discussion

### 5.1. Particle size distribution

As observed in SEM images (Fig. S1), magnetic particles used in this work are spherical in shape and relatively polydisperse. Table 1 contains results from fitting experimental size data to a Log-normal distribution:

$$f(x) = \frac{A}{\sqrt{2\pi}x\sigma} \exp \frac{-(\ln x - \mu)^2}{2\sigma^2} \quad (6)$$

where $\mu$ and $\sigma$ represent the mean and standard deviation of the variable's natural logarithm, respectively. From this, average values for particle diameters are estimated as follows: 805 ± 10 nm for iron and 90.6 ± 1.2 nm for magnetite. Histograms corresponding to magnetic particles are shown in Fig. S2.

Particle size affects in different ways to adsorption and magnetic separation phenomena. On the one hand, a large particle size is required to enhance magnetic separation under the presence of a magnetic field; large particles interact more strongly under the presence of the field moving towards magnetic field gradients. On the other hand, an important drawback comes from the fact that these particles are expected to quickly sediment under gravity. As a way of example, according to Stokes equation, an isolated one micronsized iron particle (density 7500 $kg\,m^{-3}$) immersed in water (25 °C, 1 mPa s) reaches a terminal velocity of 3.6 $\mu m\,s^{-1}$.

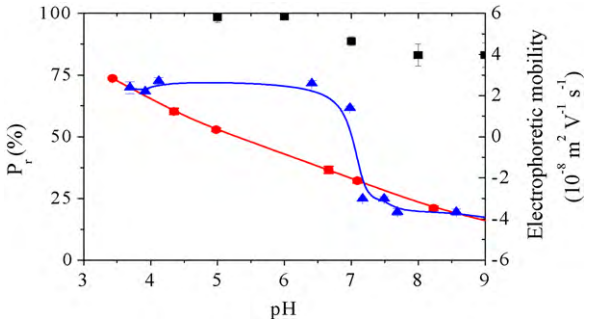


**Fig. 1.** Effect of pH on the efficiency of P removal, $P_r$ (%) and on the electrophoretic mobility of iron particles. Squares indicate P removal. Circles and triangles indicate electrophoretic mobility for bare and APTS-coated iron particles, respectively. The standard deviation is represented by vertical bars. Lines are plotted to guide the eye.

Furthermore, another important challenge is the fact that a larger adsorption requires small absorbents since surface/volume ratio strongly increases when decreasing the particle size. In conclusion, from a particle size investigation, bare magnetite particles are expected to have larger adsorption capacity if compared to iron ones. However, larger magnetic field gradients would be required for magnetite removal from solution.

### 5.2. Magnetic characterization

Typical hysteresis curves obtained for iron and magnetite powders are shown in Fig. S3 for magnetic fields in the range from −1500 to 1500 $kA\,m^{-1}$. As observed, for iron particles a ferromagnetic behavior is found with a negligible remnant magnetization as expected from a soft magnetic system. This result suggests that particles are multidomain having a saturation magnetization of 1725 $kA\,m^{-1}$ in close agreement with the bulk value 1720 $kA\,m^{-1}$ [29]. Qualitatively similar results are obtained for magnetite ($Fe_3O_4$) because of its ferrimagnetic order due to an inverse spinel crystalline structure. As expected, magnetite saturation magnetization is about three times lower than iron (477 $kA\,m^{-1}$ at 300 K).

### 5.3. Electrokinetic behavior

Iron particles used here do present a thin oxide surface layer [30] and hence behave as amphoteric solids with surface charges controlled by the pH in the aqueous medium [31]. Fig. 1 shows electrophoretic mobility of iron particles as a function of pH. An isoelectric point around pH 6.5 is found, in good agreement with previously reported data on iron oxide-based colloids [32,33]. At low pH values the particles are expected to be positively charged. On the contrary, at high pH values they are expected to bear a negative charge. As a consequence, in the case that the adsorption process is dominated by electrostatic interactions, low pH's would be required for phosphate removal from solution.

### 5.4. Effect of pH on P removal from Fe-based aqueous solution

P removal is an index frequently used for quantifying the efficiency of an adsorption method [34,35]. P removal efficiency (in %), $P_r$, is defined as the ratio between the adsorbed P concentration to the initial P concentration:

$$P_r = \frac{C_0 - C_e}{C_0} \times 100 \quad (7)$$

In Fig. 1 we show results for $P_r$ at different pH's for Fe suspensions. As observed, iron magnetic particles do behave as excellent adsorbents for phosphate; whatever the pH, the efficiency is larger than 80% (very similar results were found for magnetite). These

values are in the range of those reported in the literature for similar pH conditions using other P adsorbents. For example, Robb et al. [34] estimated an average P reduction around 90% when using Phoslock (a modified clay) for P removal from wastewaters. Similarly, Dixon [36] quantified P removal efficiencies near 85% when using magnetite. And, more recently, Ou et al. [35] found that lanthanum-doped mesoporous $SiO_2$ was able to remove nearly 100% of the initial P. However, it is worthy to note that the last authors used initial P concentrations 3 times lower than that used in the present study. Finally, much lower P removal efficiencies are also reported in the literature. Therefore, Shaikh and Dixit [37] quantified P removal efficiencies down to 10% at pH 7 when using aluminium sulfate and magnetite as adsorbents, measuring the highest efficiencies at pH 4 (~90%).

Our results showed a slight decrease in P removal efficiency with increasing pH (cf. Fig. 1). They are in agreement with those observed by Dixon [36] from pH 6 to pH 9, while a notable decrease in P removal was detected by this author at higher pH's. The slight decrease in P removal observed in this study, from pH 5 to pH 9, could be qualitatively explained through electrophoretic mobility curves shown in Fig. 1. These results suggest that the adsorption mechanism is not purely electrostatic [38] since negatively charged Fe particles still do adsorb a very significant amount of P. However, the investigation of the mechanisms governing the adsorption of P on the particles is out of the scope of this paper (for more information see [38]). Similarly to our results, Illés and Tombácz [39] observed that magnetite was an excellent adsorbent for humic acids despite of the electrostatic repulsion at pH ~ 9. More recently, Borgnino et al. [40] showed that despite the negative electrophoretic mobility of two Fe (III)-modified montmorillonites, they were good P adsorbents. The fact the P adsorption is so efficient independently on the pH reinforces the idea of using magnetic particles as P adsorbents for lake restoration. As natural waters are commonly from neutral to basic, it is difficult to find good adsorbent materials, mainly because the isoelectric points of most frequently oxides are around this value. In our case, magnetic particles do behave exceptionally well even at pH 7 where the P removal efficiency was larger than 85%.

### 5.5. Adsorption isotherms: comparing P adsorption capacity between Fe and $Fe_3O_4$ particles

Adsorption isotherms ($q$ versus $C_e$ plots) were measured for bare iron and magnetite particles. Results are shown in Fig. 2. P maximum adsorption capacity ($M_L$) was estimated by fitting the experimental data to Langmuir isotherm, and revealed interesting differences between the two particles employed. Comparison between micronsized iron and nanosized magnetite particles evidenced the higher P adsorption capacity of magnetite ($M_L = 27.15\ mg\ g^{-1}$) if compared to iron particles ($M_L = 18.83\ mg\ g^{-1}$). In particular for an initial SRP concentration of $35\ mg\ P\ L^{-1}$, the P adsorption was 1.4 times higher for the magnetite than for iron particles. These results could be explained in terms of the different particle size between iron and magnetite (cf. Fig. S2). A larger adsorption is expected for magnetite if compared to iron because magnetite particles are smaller than iron ones, hence increasing the available surface for adsorption. For practical applications, it is essential to remark that as Daou et al. [38] observed, phosphatation does not modify the structure and the magnetization of magnetite assuring its efficient removal once added to aqueous solutions.

### 5.6. Reusability of magnetic micro- and nanoparticles

A new challenge for using magnetite particles is their reutilization and therefore, optimizing the economic cost. In fact, although

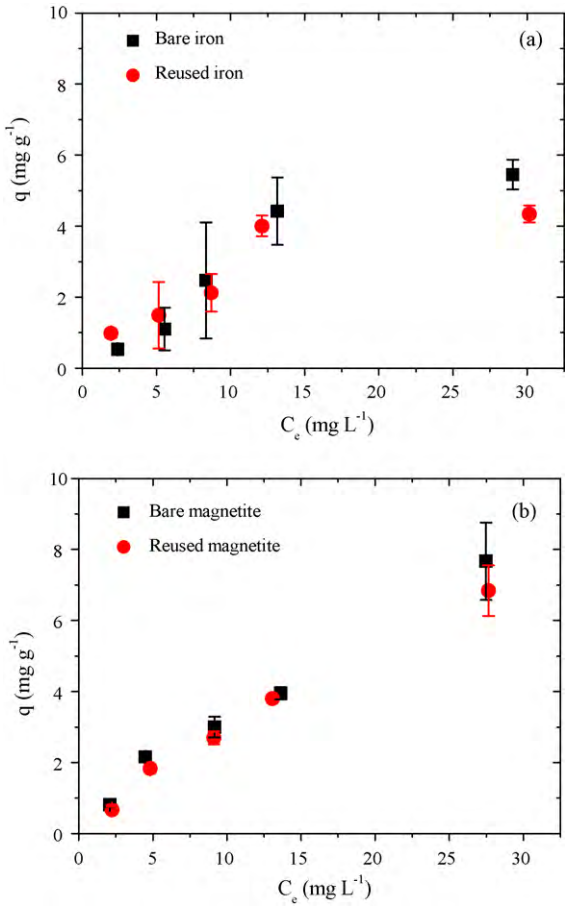


**Fig. 2.** P adsorption on bare and reused iron (a) and magnetite (b) particles.

the use of both iron and magnetite particles could not be cost-effective in a full-scale process, the particles reutilization makes this method especially interesting for lake restoration due to the large water volume to be treated.

Results obtained in this work suggest that when re-using particles that had already adsorbed P, by washing them with NaOH, P adsorption capacity of reused particles experienced a slight change whatever the magnetic particles involved (Fig. 2). In particular, a slight decrease in the empirical saturation constant is observed for iron particles (from 18.83 to $15.80\ mg\ g^{-1}$) and for magnetite particles (from 27.15 to $23.83\ mg\ g^{-1}$). Indeed, for an initial SRP concentration of $35\ mg\ P\ L^{-1}$, the P adsorption was reduced 20% for reusable iron particles and for an initial SRP concentration of $3\ mg\ P\ L^{-1}$, the P adsorption was reduced 18% for reusable magnetite particles. In conclusion, the possibility of re-using magnetic particles opens new perspectives in the search for practical applications significantly reducing economic costs.

### 5.7. Adsorption and P removal efficiency by using magnetic functionalized particles

One of the main difficulties facing almost all the novel techniques based on using magnetic nanoparticles is their tendency to aggregate [41]. As aggregation reduces the specific surface area and the interfacial free energy [42,43], it is expected that adsorption properties are likely to be diminished. The principal cause of aggregation is generally assumed to be the short-range van der Waals attraction and/or remnant magnetization forces between the particles. To counteract these attractive interactions and promote kinetic stability, the surface of magnetite and iron particles can

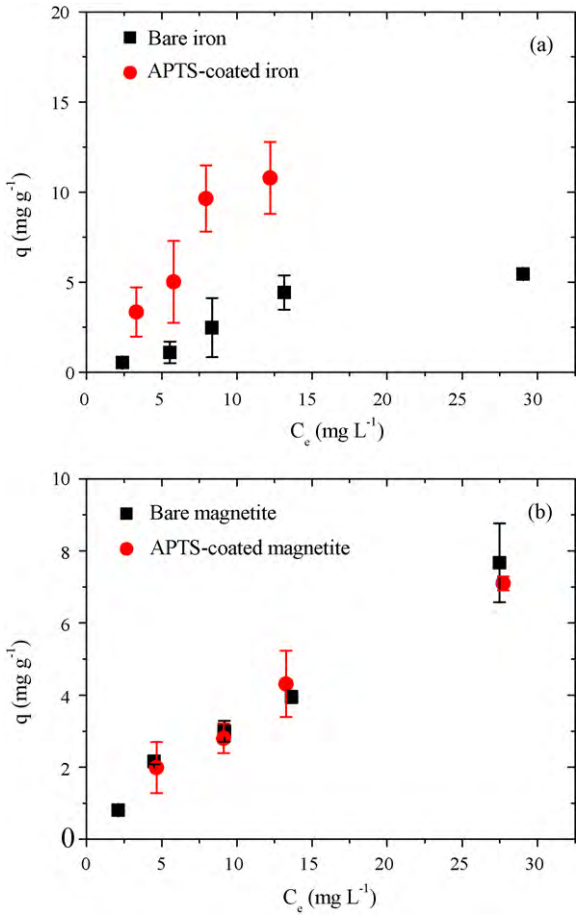


**Fig. 3.** P adsorption on bare and on APTS-coated iron (a) and magnetite (b) particles.

be modified by attaching polymers, organic long-chain molecules or designing more complex composite materials to improve the affinity of the particles for specific target species [26,44–46].

In this work, to further understand the effect of electrostatic interactions in the adsorption mechanism, magnetite and iron particles were coated with amino silane groups as detailed in the experimental section. These $-NH_2$ groups would provide the particles with a positive charge hence increasing adsorption capacity. Actually, preliminary electrophoretic mobility measurements demonstrate that particles become positively charged over a larger pH range having also a larger net surface charge (see Fig. 1).

Adsorption tests show that when coating iron particles with APTS, a notable increase in P maximum adsorption capacity ($M_L$) is found from 18.83 mg $g^{-1}$ (uncoated iron particles) to 25.06 mg $g^{-1}$ (APTS-coated iron particles) (Fig. 3). Indeed, the higher P adsorption properties of APTS-coated iron particles compared to uncoated particles could be explained by a notable increase in electrophoretic mobility, as it is mentioned above. Therefore, uncoated particles experienced electrophoretic mobility values of $-2.14 \times 10^{-8}$ $m^2$ $V^{-1}$ $s^{-1}$ at pH 7.09 while APTS-coated iron particles show electrophoretic mobility values of $1.4 \times 10^{-8}$ $m^2$ $V^{-1}$ $s^{-1}$ at pH 6.98 (Fig. 1). The effect of APTS-coating on P maximum adsorption capacity was less pronounced for the case of magnetite particles, where similar maximum adsorption capacities were observed in uncoated and coated particles.

## 6. Conclusions

This study provides a quantitative estimate showing the convenience of using iron and magnetite particles for removing P from solution. An important requisite for the magnetic components is their biocompatibility and low toxicity. Iron and magnetite are well known magnetic materials that accomplish this requirement. Although magnetite particles adsorb more P than iron particles as a consequence of the different particle size, APTS-coated iron particles were especially efficient for P removal. In addition, the existence of similar P adsorption capacities in bare and in reused magnetite and iron particles makes this method especially interesting for applying in a full-scale process for lake restoration. In particular, we think that the use of magnetic separation technology could be useful for decreasing P external loading to aquatic ecosystems by constructing artificial ponds where adding iron particles and retaining P before entering the lake. However, we put forward the need for future research focused on a better understanding of the adsorption mechanisms involved as well as the study of the potential interference in P adsorption caused by anions and cations present in solution.

## Acknowledgements

The authors would like to thank F. Galisteo-González for providing the Bool2k software used for the generation of particle size distributions from SEM micrographs. This work was supported by an Integrated Action Project “Acción Integrada (2953/07)” from the University of Granada and MICINN MAT 2009-14234-C03-03 project (Spain).

## Appendix A. Supplementary data

Supplementary data associated with this article can be found, in the online version, at doi:10.1016/j.jhazmat.2010.05.020.

## References

[1] OCDE, Eutrophisation des eaux. Metodes de surveillance d'evaluation et de lutte, París, 1982.
[2] H. SAS, Lake Restoration by Reduction of Nutrient Loading: Expectations, Experiences, Extrapolations, Akademia Verlag Richarz, Sankt Augustin, 1989.
[3] D.G. Cooke, E.B. Welch, S.A. Peterson, S.A. Nicholas, Restoration and Management of Lakes and Reservoirs, CRC Press, Boca Raton, 2005.
[4] M. Hupfer, S. Hilt, Lake restoration, in: S.E. Jørgensen, B.D. Fath (Eds.), Encyclopedia of Ecology, Vol.3, Elsevier, Oxford, 2008, pp. 2080–2093.
[5] V.H. Smith, Eutrophication, in: G.E. Likens (Ed.), Encyclopedia of Inland Waters, vol. 3, Elsevier, Oxford, 2009, pp. 61–73.
[6] M. Søndergaard, E. Jeppensen, T.L. Lauridsen, Ch. Skov, E.H. van Nes, R. Roijackers, E. Lammens, R. Portielje, Lake restoration: successes, failures and long-term effects, J. Appl. Ecol. 44 (2007) 1095–1105.
[7] R.D. Gulati, L.M.D. Pires, E. Van Donk, Lake restoration studies: failures, bottlenecks and propects of new ecotechnological measures, Limnologica 38 (2008) 233–247.
[8] E. Jeppesen, M. Søndergaard, H.S. Jensen, A.M. Ventäla, Lake and reservoir management, in: G.E. Likens (Ed.), Encyclopedia of Inland waters, Vol.1, Elsevier, Oxford, 2009, pp. 295–309.
[9] Ch.M. Chang, Y.J. Wang, C. Lin, M.K. Wang, Novel predicting methods for the removal of divalent metal ions by magnetite/amorphous iron oxide composite systems, Colloids Surf. A: Physicochem. Eng. Aspects 234 (2004) 1–7.
[10] J. Hu, I.M.C. Lo, G. Chen, Removal of Cr (VI) by magnetite nanoparticle, Water Sci. Technol. 50 (2004) 139–146.
[11] N.A. Booker, D. Keir, A. Priestley, C.D. Rithchie, D.L. Sudarmana, M.A. Woods, Sewage clarification with magnetite particles, Water Sci. Technol. 123 (1991) 1703–1712.
[12] K.S. Sing, Ground water monitor, Technol. Profile 21 (1994) 60.
[13] I. Safarik, M. Safarikova, V. Buricova, Sorption of water soluble organic dyes on magnetic poly(oxy-2, 6- dimethyl-1,4-phenylene, Collect. Czech. Chem. Commun. 60 (1995) 1448–1456.
[14] J.D. Orbell, L. Godhino, S.W. Bigger, T.M. Nguyen, L.N. Ngeh, Oil spill remediation using magnetic particles, J. Chem. Edu. 74 (1997) 1446.
[15] J.M. Ginder, Rheology controlled by magnetic fields, Encyclopedia Appl. Phys. 16 (1996) 487–503.
[16] T. Rheinlander, R. Kotitz, W. Weitschies, W. Semmler, Magnetic fractionation of magnetic fluids, J. Magn. Magn. Mater. 219 (2000) 219–228.
[17] L. Moore, A. Rodriguez, P. Williams, B. McCloskey, M. Nakamura, J. Chalmers, M. Zborowski, Progenitor cell isolation with a high-capacity quadrapole magnetic flow sorter, J. Magn. Magn. Mater. 225 (2001) 277–284.

[18] R. Massart, Preparation of aqueous magnetic liquids in alkaline and acidic media, IEEE Trans. Magnet. 17 (1981) 1247–1248.
[19] R.E. Rosensweig, Ferrohydrodynamics, Cambridge University Press, Dover, 1985.
[20] T. Sugimoto, E.J. Matijevic, Formation of uniform spherical magnetite particles by crystallization from ferrous hydroxide gels, Colloid Interface Sci. 74 (1980) 227–243.
[21] J. de Vicente, A.V. Delgado, R.C. Plaza, J.D.G. Durán, F. González-Caballero, Stability of cobalt ferrite colloidal particles. effect of pH and applied magnetic fields, Langmuir 16 (2000) 7954–7961.
[22] N. Karapinar, E. Hoffmann, H. Hahn, Magnetite seeded precipitation of phosphate, Water Res. 38 (2004) 3059–3066.
[23] J. Murphy, J.P. Riley, A modified single solution method for the determination of phosphate in natural waters, Anal. Chim. Acta 27 (1962) 31–36.
[24] A. del Campo, T. Sen, J.P. Lellouche, I.J. Bruce, Multifunctional magnetite and silica-magnetite nanoparticles: synthesis, surface activation and applications in life sciences, J. Magn. Magn. Mater. 293 (2005) 33–40.
[25] E. Tombácz, in: J. Tóth (Ed.), Adsorption: Theory, Modelling and Analysis, Decker, New York, 2002, p. 711.
[26] M.E. Essington (Ed.), Soil and Water Chemistry, CRC Press, Boca Raton, Florida, 2004, p. 534.
[27] D.F. Evans, H. Wennestrom (Eds.), The Colloidal Domain; Where Physics, Chemistry, Biology and Technology Meet, Wiley-VCH, New York, 1994, p. 170.
[28] StatSoft Inc. Statistica for Windows (computer program manual). StatSoft Inc., Tulsa, 1997.
[29] E. Trémolet de Lacheisserie, Magnétisme, Presses Universitaires de Grenoble, Grenoble, France, 1999.
[30] J. de Vicente, G. Bossis, S. Lacis, M. Guyot, Permeability measurements in cobalt ferrite and carbonyl iron powders and suspensions, J. Magn. Magn. Mater. 251 (2002) 100–108.
[31] R.J. Hunter, Foundations of Colloid Science, Oxford University Press Inc., New York, 2002.
[32] A.E. Regazzoni, M.A. Blesa, A.J.G. Maroto, Interfacial properties of zirconium dioxide and magnetite in water, J. Colloid Interface Sci. 91 (1983) 560–570.
[33] M. Kosmulski, pH-dependent surface charging and points of zero charge, III. Update, J. Colloid Interface Sci. 298 (2006) 730–741.
[34] M. Robb, B. Greenop, Z. Goss, G. Douglas, J. Adeney, Application of Phoslock™, an innovative phosphorus binding clay, to two Western Australian waterways: preliminary findings, Hydrobiologia 494 (2003) 237–243.
[35] E. Ou, J. Zhou, S. Mao, J. Wang, F. Xia, L. Min, Highly efficient removal of phosphate by lanthanum-doped mesoporous $SiO_2$, Colloids Surf. A: Physicochem. Eng. Aspects 308 (2007) 47–53.
[36] D.R. Dixon, Colour and turbidity removal with reusable magnetite particles-VII, Water Res. 18 (1984) 529–534.
[37] A.M.H. Shaikh, S.G. Dixit, Removal of phosphate from waters by precipitation and high gradient magnetic separation, Water Res. 26 (1992) 845–852.
[38] T.J. Daou, S. Begin-Colin, J.M. Grenéche, F. Thomas, A. Derory, P. Bernhardt, P. Legaré, G. Pourroy, Phosphate adsorption properties of magnetite-based nanoparticles, Chem. Mater. 19 (2007) 4494–4505.
[39] E. Illés, E. Tombacz, The role of variable surface charge and surface complexation in the adsorption of humic acid on magnetite, Colloids Surf. A: Physicochem. Eng. Aspects 230 (2004) 99–109.
[40] L. Borgnino, M.J. Avena, C.P. de Pauli, Synthesis and characterization of Fe (III)-montmorillonites for phosphate adsorption, Colloids Surf. A: Physicochem. Eng. Aspects 341 (2009) 46–52.
[41] A. Zhu, L. Yuan, T. Liao, Suspension of $Fe_3O_4$ nanoparticles stabilized by chitosan and o-carboxymethylchitosan, Int. J. Pharmaceut. 350 (2008) 361–368.
[42] D.W. Elliott, W.X. Zhang, Field assessment of nanoscale biometallic particles for groundwater treatment, Environ. Sci. Technol. 35 (2001) 4922–4926.
[43] G. Pan, L. Li, D. Zhao, H. Chen, Immobilization of non-point phosphorus using stabilized magnetite nanoparticles with enhanced transportability and reactivity in soils, Environm. Pollut., doi:10.1016/j. envpol.2009.08.003.
[44] Y.C. Chang, S.W. Chang, D.H. Chen, Magnetic chitosan nanoparticles: studies on chitosan binding and adsorption of Co (II) ions, React. Funct. Polym. 66 (2006) 335–341.
[45] M. Ma, Y. Zhang, W. Yu, H.-Y. Shen, H.-Q. Zhang, N. Gu, Preparation and characterization of magnetite nanoparticles coated by amino silane, Colloids Surf. A: Physicochem. Eng. Aspects 212 (2003) 219–226.
[46] J. Zhi, Y.L. Wang, Y.C. Lu, J.Y. Ma, G.S. Luo, In situ preparation of magnetic chitosan/$Fe_3O_4$ composite nanoparticles in tiny pools of water-in-oil microemulsion, React. Funct. Polym. 66 (2006) 1552–1558.